IUST
Iran University of Science and Technology

Iranian Journal of Electrical and Electronic Engineering

Journal Homepage: ijeee.iust.ac.ir

Research Paper

Coordinated Control of LFC and SMES in the Power System Using a New Robust Controller

F. Amiri* and M. H. Moradi*(C.A.)

Abstract: In this paper, a coordinated control method for LFC and SMES systems based on a new robust controller is designed. The proposed controller is used to compensate for frequency deviations related to the power system, to prevent excessive power generation in conventional generators during load disturbances, and to reduce power fluctuations from wind power plants. The new robust controller does not require the measurement of all the power system states and it only uses the output feedback. It also has a higher degree of freedom than the conventional robust controllers (conventional output feedback) and thus it helps improve the system control. The proposed control method is highly robust against load and distributed generation resources (wind turbine) disturbances and it is also robust against the uncertainty of the power system parameters. The proposed method is compared under several scenarios with the coordinated control method for LFC and SMES systems based on Moth Swarm Algorithm-optimized PID controller, the LFC system based on Moth Swarm Algorithm-optimized PID controller with SMES, the coordinated control method for LFC and SMES systems based on Robust Model Predictive Control, and the LFC system based on optimized PID controller without SMES and it puts on satisfactory performance. The simulation was performed in MATLAB.

Keywords: Robust Controller, Load-Frequency Control, Coordinated Control, Uncertainty of the Power System.

1 Introduction

WITH the growth of urbanization and industrialization of cities, the need for electric power has increased. As a result, many alternative energy resources such as wind turbines and photovoltaic (PV) systems penetrated the power systems. Despite the availability of these resources, the complicated control and inaccuracy of systems have increased [1, 2]. The increase in the penetration of alternative energy resources has advantages such as increased electric power and supply of power to remote areas. However, these resources have created a new challenge, which raises this question: Can these resources operate with stability next to the existing generation resources [3-5]? Moreover, frequency control is among the major challenges posed by the penetration of distributed generation resources in power systems [6]. If the disturbance is caused in a power system, which disturbs the balance between generation and consumption, there will be frequency oscillations. For instance, if the load suddenly increases, the frequency falls below the nominal value, which leads to frequency instability if it is not controlled. The primary control loop is the first control loop that limits the frequency decline after the occurrence of disturbance and prevents frequency instability [7]. This primary control loop is typically installed on a synchronous generator. The primary loop only limits the frequency deviations and the frequency deviations do not equal zero in the presence of disturbances. A secondary controller (LFC) is used to reduce the frequency error to zero in the presence of disturbance [8-10]. The penetration of distributed generation resources such as wind turbines in power systems reduces the power system's total inertia, and if a disturbance occurs (load

Iranian Journal of Electrical and Electronic Engineering, 2021.
Paper first received 13 June 2020, revised 01 March 2021, and accepted 06 March 2021.
* The authors are with the Department of Electrical Engineering, Bu-Ali Sina University, Hamedan, Iran.
E-mails: f.amiri94@basu.ac.ir and mh_moradi@yahoo.co.uk.
Corresponding Author: M. H. Moradi.
https://doi.org/10.22068/IJEEE.17.4.1912

and distributed generation resources), the frequency deviations increase. The complexity of the load-frequency control problem increases due to the increase in the frequency deviations in the power system with wind turbines. Various control methods have also been employed for load-frequency control (LFC) in power systems with wind turbines [12-28].

In [12], a sliding mode controller is designed for the load frequency control system in power systems with the wind turbine. In [13], a neural network based on sliding mode control is designed for the load frequency control system in power systems with wind turbines. The control methods proposed in [12, 13] for load-frequency control in power systems are partly robust against disturbance and the uncertainty of the power system parameters. However, if the uncertainty of the power system parameters increases, this controller does not stage a satisfactory performance. In [14-16], a model predictive controller is designed for the load frequency control system in power systems with wind turbines. The model predictive controller is robust against the load and distributed generation resources disturbance. However, this controller does not put on a satisfactory performance under the uncertainty of power system parameters. In [17], a Fractional order PID (FOPID) controller is designed for the load frequency control system in power systems with wind turbines. The FOPID controller shows less sensitivity to the variations of the power system parameters than the PID controller because it has two degrees of freedom. However, it does not put on satisfactory performance in the attenuation of the load and distributed generation resources disturbance. The load-frequency control system in a power system with a wind turbine requires controllers that are robust against the uncertainty of parameters and can considerably weaken the disturbance effect (load and distributed generation resources). In [18], a fuzzy PID controller is designed for the load frequency control system in power systems with wind turbines. In [19, 20], the optimized PID controller is designed for the load frequency control system in power systems with the wind turbine. The PID controllers are still used in industries and power systems due to their simple structure. These types of controllers do not perform properly under the effect of disturbance attenuation. Energy storage systems are not used in the control systems proposed for the power systems with wind turbines [12-20]. Energy storage systems such as Superconducting Magnetic Energy Storage (SMES) have advantages such as higher efficiency, increased lifetime, and faster response over the other energy storage systems [21-23]. The presence of these energy storage systems in power systems improves frequency stability. In [23-26], a coordinated control method for load-frequency and SMES is designed based on different controllers to reduce the frequency oscillations resulting from the load and distributed generation resources disturbance in power systems. In [24], a coordinated control method for the LFC and SMES systems based on the neural-fuzzy controller is designed for power systems. Besides, the coordinated control method for LFC and SMES systems based on the Particle swarm optimization (PSO)-optimized PID is designed for power systems in [25]. In [26], the coordinated control method for LFC and SMES systems based on the Moth Swarm Algorithm (MSA)-optimized PID controller is designed for power systems. In [27, 28], the Robust Model Predictive Control (RMPC) controller is designed to control the voltage and frequency in the power system.

The controllers used in the power system for coordinated control method for LFC and SMES systems do not have a high attenuation capacity due to disturbances (caused by load and distributed generation sources) [23-26]. These control methods are also not robust to the uncertainty of system parameters [23-26], so it is necessary to have a proper control method in the power system that can greatly reduce the disturbances in the power system and also be robust to the uncertainty of parameters. The proposed method in this paper is a new method (new output feedback) in robust control that has more degrees of freedom, the choice of degrees of freedom of the proposed controller (ϕ_1, ϕ_2, and ϕ_3) is the responsibility of the designer. The proposed method is used to coordinate the LFC and SMES system in the power system in order to maintain the frequency stability of the power system in the presence of distributed generation sources. The proposed controller parameters are obtained by solving linear matrix inequalities in MATLAB Yalmip. To show the effective performance of the proposed control method in improving the frequency stability of the power system has been compared with several control methods in this field.

This paper consists of several sections: in section two of this paper, the structure of the power system with a wind turbine is described. In section three, the proposed new controller is introduced and proven. Section four presents the simulation. Section five presents the conclusions.

2 Structure of the Power System

2.1 System Components

Fig. 1 shows the structure of the power system. The studied power system includes several hydropower plants, several non-reheat power plants, several reheat power plants, several wind turbines, several energy storage systems (ESS), and different loads. The total amount of power produced in the studied power system is 38000 MW, while the peak load is 29000 MW [24-26]. Fig. 2 shows the dynamic model of the study power system in which different components are modeled using the reduced-order model, which suits the stability analysis of frequency [1, 2]. As seen in Fig. 2, a coordinated control method for LFC and SMES systems

based on a new robust controller to improve the frequency deviations caused by the load and distributed generation resources (wind turbines) disturbance. Generation rate limitations are defined for different power plants to increase the accuracy of the dynamic model of the power system. The SMES dynamic model is a first-order linear model, while the wind turbine dynamic model is a nonlinear model. The wind turbine nonlinear dynamic model is depicted in Fig. 3 concerning the random wind speed. The study power system parameters are also listed in Appendix 1 [24-26].

2.2 Space State of the Studied Power System

To design the proposed controller for the coordinated control of the LFC and SMES systems in the studied power system, the system state space is shown according to (1) and (2) [22, 25]. In (1) and (2), Δf is the power system frequency deviation. ΔP_{Non_Reh} is the generated power from the non-reheat power plant, ΔP_{Reh} is the generated power from the reheat power plant, ΔP_{g2} is the generated from the governor 2, ΔP_{g3} is the generated from the governor 3, ΔP_{Hydro} is the generated power from the hydropower plant, ΔP_L is the load power, ΔP_{SMES} is the generated power from the superconducting magnetic energy.

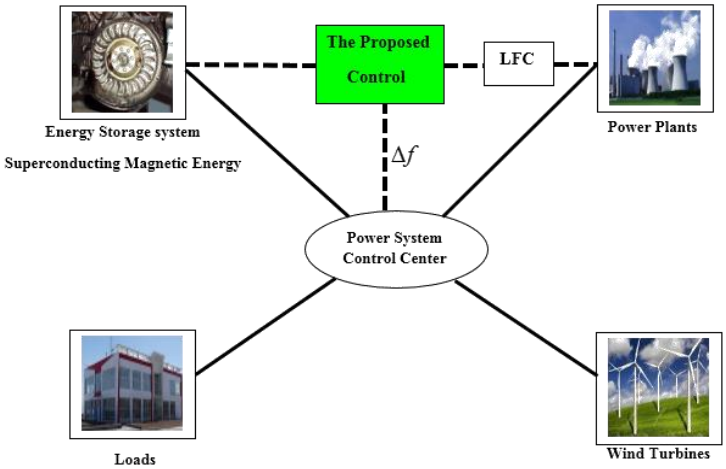

Fig. 1 Structure of the power system.

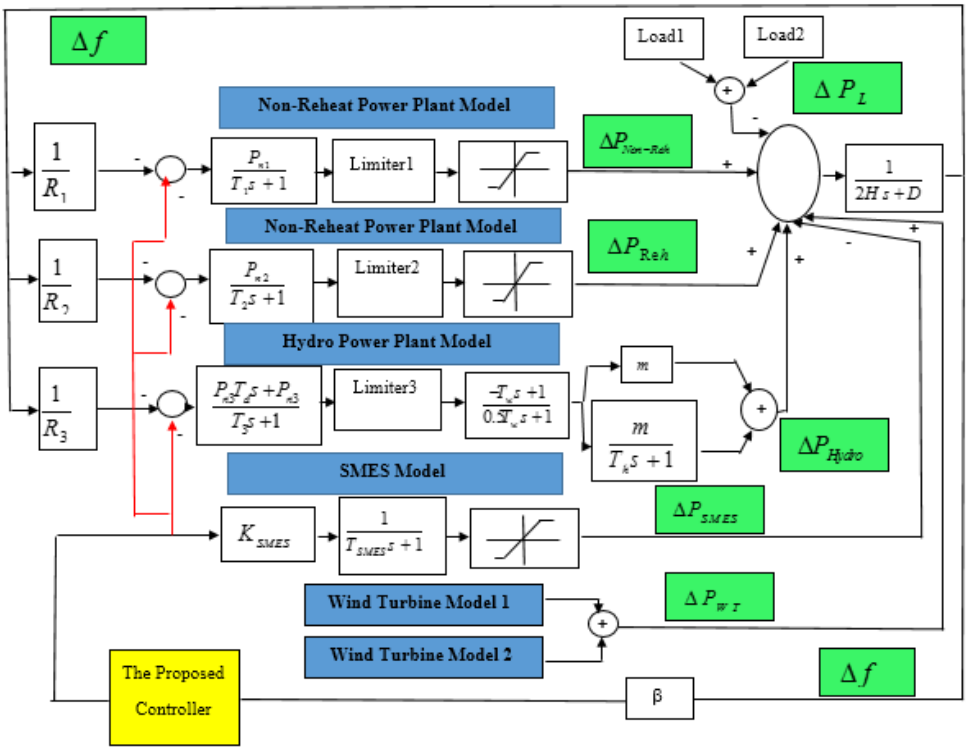

Fig. 2 The dynamic model of the study power system [24-26].

3 Designing a New Robust Controller for Coordinated Control of LFC and SMES Systems

3.1 The Proposed Controller Structure

In this section, the new robust control method has been designed for the studied power system. The controller structure is designed in such a way that there is uncertainty of parameters and disturbance in the studied power system. Also, we cannot measure all states and modes, and even if can, it will cost more due to the need for more sensors. The control system is designed in such a way that the power system would be free of external disturbances and under the uncertainty

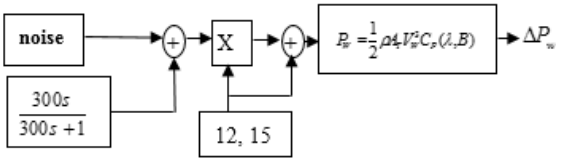

Fig. 3 The wind turbine nonlinear dynamic model [26].

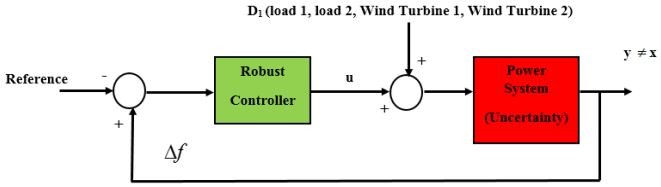

Fig. 4 The power system structure with the proposed controller.

$$\begin{bmatrix} \dot{\Delta f} \\ \dot{\Delta P}_{Non-reh} \\ \dot{\Delta P}_{Reh} \\ \dot{\Delta P}_{g2} \\ \dot{\Delta P}_{Hedro} \\ \dot{\Delta P}_{g3} \\ \dot{\Delta P}_{WT} \\ \dot{\Delta P}_{SMES} \end{bmatrix} = \begin{bmatrix} -\frac{D}{2H} & \frac{1}{2H} & \frac{1}{2H} & 0 & \frac{1}{2H} & 0 & \frac{1}{2H} & \frac{1}{2H} \\ -\frac{P_{n1}}{T_1R_1} & -\frac{1}{T_1} & 0 & 0 & 0 & 0 & 0 & 0 \\ -\frac{mP_{n2}}{T_2R_2} & 0 & -\frac{1}{T_h} & \frac{2m}{T_h}-\frac{m}{T_2} & 0 & 0 & 0 & 0 \\ -\frac{P_{n2}}{T_2R_2} & 0 & 0 & -\frac{1}{T_2} & 0 & 0 & 0 & 0 \\ \frac{-T_dP_{n3}D}{T_3R_3H}+\frac{2P_{n3}}{T_3R_3} & \frac{T_dP_{n3}}{T_3R_3H} & \frac{T_dP_{n3}}{T_3R_3H} & 0 & \frac{T_dP_{n3}}{T_3R_3H}-\frac{2}{T_w} & \frac{2}{T_w}+\frac{2}{T_3} & 0 & 0 \\ \frac{T_dP_{n3}D}{2T_3R_3H}-\frac{P_{n3}}{T_3R_3} & -\frac{T_dP_{n3}}{2T_3R_3H} & -\frac{T_dP_{n3}}{2T_3R_3H} & 0 & -\frac{T_dP_{n3}}{2T_3R_3H} & -\frac{1}{T_3} & 0 & 0 \\ 0 & 0 & 0 & 0 & 0 & 0 & -\frac{1}{T_{WT}} & 0 \\ 0 & 0 & 0 & 0 & 0 & 0 & 0 & -\frac{1}{T_{SMES}} \end{bmatrix} \times$$

$$\begin{bmatrix} \Delta f \\ \Delta P_{Non-reh} \\ \Delta P_{Reh} \\ \Delta P_{g2} \\ \Delta P_{Hedro} \\ \Delta P_{g3} \\ \Delta P_{WT} \\ \Delta P_{SMES} \end{bmatrix} + \begin{bmatrix} 0 \\ -\frac{P_{n1}}{T_1} \\ -\frac{mP_{n2}}{T_2} \\ -\frac{P_{n2}}{T_2} \\ \frac{2P_{n3}}{T_3} \\ \frac{-P_{n3}}{T_3} \\ 0 \\ \frac{-K_{SMES}}{T_{SMES}} \end{bmatrix} [u] + \begin{bmatrix} 0 & -\frac{1}{2H} \\ 0 & 0 \\ 0 & 0 \\ 0 & 0 \\ 0 & -\frac{T_dP_{n3}}{T_3R_3H} \\ 0 & \frac{T_dP_{n3}}{2T_3R_3H} \\ -\frac{1}{T_{WT}} & 0 \\ 0 & 0 \end{bmatrix} \begin{bmatrix} \Delta P_{wind} \\ \Delta P_L \end{bmatrix} \quad (1)$$

$$\mathbf{y}=\begin{bmatrix}1 & 0 & 0 & 0 & 0 & 0 & 0 & 0\end{bmatrix}\begin{bmatrix}\Delta\mathbf{f}\\ \Delta\mathbf{P}_{\mathbf{Non\text{-}reh}}\\ \Delta\mathbf{P}_{\mathbf{Reh}}\\ \Delta\mathbf{P}_{\mathbf{g2}}\\ \Delta\mathbf{P}_{\mathbf{Hedro}}\\ \Delta\mathbf{P}_{\mathbf{g3}}\\ \Delta\mathbf{P}_{\mathbf{WT}}\\ \Delta\mathbf{P}_{\mathbf{SMES}}\end{bmatrix} \tag{2}$$

of parameters with an asymptote stable output feedback and can meet the $\frac{\|\mathbf{z}\|_{L_2}}{\|\mathbf{w}\|_{L_2}}\le\gamma$ criterion in the presence of disturbances in the power system. The structure of the power system (with parameter uncertainty and under disturbance) with the proposed dynamic controller is shown in Fig. 4. In Fig. 4, *y* is the Frequency deviation of the power system. D_1 is disturbance entering the power system and *u* is the control signal. The dynamics of the power system are modeled by considering the regulated output (*Z*) as (3) [29].

$$\begin{aligned}\dot{\mathbf{x}}&=\mathbf{A}_{\mathbf{n\times n}}(\mathbf{t})\mathbf{x}_{\mathbf{n}\times 1}+\mathbf{B}_{\mathbf{n\times m}}(\mathbf{t})\mathbf{u}_{\mathbf{m}\times 1}+\mathbf{D}_{\mathbf{n\times d}}(\mathbf{t})\mathbf{w}_{\mathbf{d}\times 1}\\ \mathbf{z}&=\mathbf{C}_{1_{\mathbf{q\times n}}}(\mathbf{t})\mathbf{x}_{\mathbf{n}\times 1}+\mathbf{D}_{11}(\mathbf{t})\mathbf{w}+\mathbf{D}_{12_{\mathbf{q\times m}}}(\mathbf{t})\mathbf{u}_{\mathbf{m}\times 1}\\ \mathbf{y}&=\mathbf{C}_2(\mathbf{t})\mathbf{x}_{\mathbf{n}\times 1}+\mathbf{D}_{21}(\mathbf{t})\mathbf{w}+\mathbf{D}_{22}(\mathbf{t})\mathbf{u}\end{aligned} \tag{3}$$

In (3), *n* is the number of state variables, *m* indicates the control inputs, *d* is the number of disturbances, *z* is the regulated output, $D_{21}(t) = D_{22}(t) = 0$. *y* is the linear system measurement output, and *q* is the number of regulated outputs [29-32]. Since in the power system, $C_2 \neq I$, the robust output feedback control has been used. The variable *z* can be selected concerning the control design criterion. In the proposed method, all the parameters of the linear system can be assumed uncertain, so it has been modeled as (4) [29, 30]. In (4), the choice of *M* and *N* parameters is the responsibility of the designer. The uncertainty given in (4) has been re-considered as in (5), wherein $F(t)$ has been taken as 1×1. The structure of the dynamic controller proposed for coordinated control of LFC and SMES in the power system has uncertainty and disturbance, which is represented as (6).

$$\begin{cases}A(t)=A+\Delta A(t)=A+\Delta A\\ B(t)=B+\Delta B(t)=B+\Delta B\\ D(t)=D+\Delta D(t)=D+\Delta D\\ C_1(t)=C_1+\Delta C_1(t)=C_1+\Delta C_1\\ D_{12}(t)=D_{12}+\Delta D_{12}(t)=D_{12}+\Delta D_{12}\\ C_2(t)=C_2+\Delta C_2(t)=C_2+\Delta C_2\end{cases} \tag{4}$$

$$\begin{cases}\Delta A_{n\times n}=M_{A_{n\times 1}}F_{1\times 1}(t)N_{A_{1\times n}}\\ \Delta D_{n\times d}=M_{D_{n\times 1}}F_{1\times 1}(t)N_{D_{1\times d}}\\ \Delta B_{n\times m}=M_{B_{n\times 1}}F_{1\times 1}(t)N_{B_{1\times m}}\\ \Delta C_{1_{q\times n}}=M_{C1_{q\times 1}}F_{1\times 1}(t)N_{C1_{1\times n}}\\ \Delta C_{2_{p\times n}}=M_{C2_{p\times 1}}F_{1\times 1}(t)N_{C2_{1\times n}}\\ \Delta D_{12_{q\times m}}=M_{D12_{q\times 1}}F_{1\times 1}(t)N_{D12_{1\times m}}\\ F_{1\times 1}^T(t)\times F_{1\times 1}(t)\pounds I, F^2(t)\pounds 1\end{cases} \tag{5}$$

$$\begin{cases}\dot{\hat{\mathbf{x}}}_{\mathbf{n}\times 1}=\hat{\mathbf{A}}_{\mathbf{n}\times\mathbf{n}}\hat{\mathbf{x}}_{\mathbf{n}\times 1}+\hat{\mathbf{B}}_{\mathbf{n}\times\mathbf{p}}\mathbf{y}_{\mathbf{p}\times 1}\\ \mathbf{u}_{\mathbf{m}\times 1}=\hat{\mathbf{C}}_{\mathbf{m}\times\mathbf{n}}\hat{\mathbf{x}}_{\mathbf{n}\times 1}\end{cases} \tag{6}$$

By combining (3) and (6), the closed-loop system structure (power system and controller) can be represented as in (7) [29-32].

$$\begin{cases}\dot{\mathbf{x}}=\mathbf{A}(\mathbf{t})\mathbf{x}+\mathbf{B}(\mathbf{t})\hat{\mathbf{C}}\hat{\mathbf{x}}+\mathbf{D}(\mathbf{t})\mathbf{w}\\ \mathbf{z}=\mathbf{C}_1(\mathbf{t})\mathbf{x}+\mathbf{D}_{12}(\mathbf{t})\hat{\mathbf{C}}\hat{\mathbf{x}}\\ \dot{\hat{\mathbf{x}}}=\hat{\mathbf{A}}\hat{\mathbf{x}}+\hat{\mathbf{B}}\mathbf{C}_2\mathbf{x}\end{cases} \tag{7}$$

In (7), if *x* and $\hat{x}$ incline toward zero, then the entire closed-loop system will be stable. Considering $\bar{x}=\begin{bmatrix}x\\ \hat{x}\end{bmatrix}_{2n\times 1}$, Eq. (7) is rewritten as (8).

$$\begin{aligned}\dot{\bar{x}}&=\begin{bmatrix}A(t) & B(t)\hat{C}\\ \hat{B}(t)C_2(t) & \hat{A}\end{bmatrix}_{2n\times 2n}\bar{x}+\begin{bmatrix}D(t)\\ 0\end{bmatrix}_{2n\times d}w_{d\times 1}\\ &=\bar{A}\bar{x}+\bar{D}w\end{aligned} \tag{8}$$

3.2 Objectives of the Control System

For the closed-loop system (the power system with disturbance and parameter uncertainty and the proposed controller), there are 2 main objectives:

1. being asymptotically stable without disturbance of the closed-loop system and under parameter uncertainty.

2. Achieving the performance of $\frac{\|\mathbf{z}\|_{L_2}}{\|\mathbf{w}\|_{L_2}}\le\gamma$ *in the*

presence of disturbance and uncertainty of the closed-loop system with the primary zero conditions.

In the present work, the Lyapunov stability criterion has been used for proving the stability of the proposed method. For this purpose, the Lyapunov stability criterion was applied to the power system with disturbance. The Lyapunov criterion and the closed-loop system structure are defined as (9). The two conditions (9.1) and (9.2) are essential for stability based on the Lyapunov criterion.

$$\mathbf{v}=\bar{\mathbf{x}}^{\mathbf{T}}\mathbf{p}\bar{\mathbf{x}}>0\Rightarrow\mathbf{p}>0 \tag{9a}$$

$$\dot{\bar{\mathbf{x}}}=\bar{\mathbf{A}}\bar{\mathbf{x}}+\bar{\mathbf{D}}\mathbf{w} \tag{9b}$$

$$\begin{aligned}\dot{\mathbf{v}}&=\dot{\bar{\mathbf{x}}}^{\mathbf{T}}\mathbf{p}\bar{\mathbf{x}}+\bar{\mathbf{x}}^{\mathbf{T}}\mathbf{p}\dot{\bar{\mathbf{x}}}\\&=\bar{\mathbf{x}}^{\mathbf{T}}\bar{\mathbf{A}}^{\mathbf{T}}\mathbf{p}\bar{\mathbf{x}}+\mathbf{w}^{\mathbf{T}}\bar{\mathbf{D}}^{\mathbf{T}}\mathbf{p}\bar{\mathbf{x}}+\bar{\mathbf{x}}^{\mathbf{T}}\mathbf{p}\bar{\mathbf{A}}\bar{\mathbf{x}}+\bar{\mathbf{x}}^{\mathbf{T}}\mathbf{p}\bar{\mathbf{D}}\mathbf{w}<0\end{aligned} \tag{9c}$$

To prove (9a), meaning that $v>0$, the matrix P, P^{-1} is defined as (10) [29-32]. Meanwhile, PP^{-1} must become an identity matrix following (11). The linearization matrix has been considered as (12). According to (12), $p\beta_1=\beta_2$. Also, from (13), the linear matrix inequality has been obtained for the first Lyapunov criterion (9a), meaning that if the linear matrix inequality (13) is bigger than zero, then the first criterion is met ($v>0$).

$$p=\begin{bmatrix}S_{n\times n} & N_{n\times n}\\ N^{T}_{n\times n} & U_{n\times n}\end{bmatrix},p^{-1}=\begin{bmatrix}R_{n\times n} & M_{n\times n}\\ M^{T}_{n\times n} & T_{n\times n}\end{bmatrix} \tag{10}$$

$$pp^{-1}=\begin{bmatrix}SR+NM^{T} & SM+NT\\ N^{T}R+UM^{T} & N^{T}M+UT\end{bmatrix},=\begin{bmatrix}I_{n\times n} & 0\\ 0 & I_{n\times n}\end{bmatrix} \tag{11}$$

$$\beta_1=\begin{bmatrix}R & I\\ M^{T} & 0\end{bmatrix},\beta_2=\begin{bmatrix}I & S\\ 0 & N^{T}\end{bmatrix} \tag{12}$$

$$\begin{aligned}\beta_1^{T}p\beta_1=\beta_1^{T}\beta_2&=\begin{bmatrix}R & M\\ I & 0\end{bmatrix}\begin{bmatrix}I & S\\ 0 & N^{T}\end{bmatrix}\\&=\begin{bmatrix}R & RS+MN^{T}\\ I & S\end{bmatrix}=\begin{bmatrix}R & I\\ I & S\end{bmatrix}>0\end{aligned} \tag{13}$$

To calculate the second Lyapunov criterion (9c) and converting it into a linear matrix inequality, Eqs. (14)-(29) has been proved.

The equation $\frac{\|z\|_{L_2}}{\|w\|_{L_2}}\le\gamma$, which is the criterion for reduction of disturbances compared to the power system's states under uncertainty, has been written in accordance with (14). The objective function has been represented as the function j, and the negativity of the function j meets the second Lyapunov criterion, i.e. $\dot{v}<0$. The upper bound for the objective function (j) has been obtained according to (15). If (16) exists, then the function j will be negative and the second Lyapunov criterion will be met. Therefore, Eq. (16) must be converted into a linear matrix inequality. Equation (16) has been converted, through substitution and Schur complement, into (17). Since P is symmetric, so $P^T=P$ and $p=\beta_2\beta_1^{-1}$ and, accordingly, Eq. (17) has converted into (18). Equations (19) and (20) have been defined in order for linearizing (18). The linearization of (18) has been demonstrated following (21). By substituting (8) and (12) in (21), Eq. (22) has been obtained.

$$\begin{cases}\int_0^{\infty}z^{T}z\;dt\le\gamma^{2}\int_0^{\infty}w^{T}w\;dt\\ j=\int_0^{\infty}(z^{T}z-\gamma^{2}w^{T}w)dt\le 0\end{cases} \tag{14}$$

$$\begin{cases}j\le\int_0^{\infty}(z^{T}z-\gamma^{2}w^{T}w)dt+v(x(\infty))-v(x(0))\\ j\le\int_0^{\infty}(z^{T}z-\gamma^{2}w^{T}w+\dot{v})dt<0\end{cases} \tag{15}$$

$$z^{T}z-\gamma^{2}w^{T}w+\dot{v}<0 \tag{16}$$

$$\delta_1=\begin{bmatrix}\bar{A}^{T}p+p\bar{A} & p\bar{D} & \begin{bmatrix}C_1^{T}(t)\\ \hat{C}^{T}D_{12}^{T}(t)\end{bmatrix}\\ \bar{D}p & \gamma^{2}I & 0\\ \begin{bmatrix}C_1(t) & D_{12}(t)\hat{C}\end{bmatrix} & 0 & -I\end{bmatrix}<0 \tag{17}$$

$$\delta_2=\begin{bmatrix}\bar{A}^{T}\beta_2\beta_1^{-1}+p\bar{A} & \bar{\beta}_1^{T}\beta_2^{T}\bar{D} & \begin{bmatrix}C_1^{T}(t)\\ \hat{C}^{T}D_{12}^{T}(t)\end{bmatrix}\\ \bar{D}\bar{\beta}_2\beta_1^{-1} & \gamma^{2}I & 0\\ \begin{bmatrix}C_1(t) & D_{12}(t)\hat{C}\end{bmatrix} & 0 & -I\end{bmatrix}<0 \tag{18}$$

Subsequently, Eq. (22), after substituting (23), has been converted into (24). The definitions of the parameters $\hat{A}$, $\hat{B}$, and $\hat{C}$ in (23) have been adopted from [29-32], and in (24), the constant parameters have been separated from the uncertain parameters by different matrices. Equation (25) has been used to calculate the upper bound for O_1 to O_{13}. The upper bounds of O_1 to O_{13} have been obtained from (26) and (27). According to (27), if $\delta_4<0$, then $\delta_3<0$ and the second Lyapunov criterion will be met. In (27), initially, the Schur complement has been used for $\bar{o}_1$, and thus it has been represented as (28). Also, for $\bar{o}_2$ to $\bar{o}_{13}$, as in (28), the Schur complement has been used so that it has been ultimately rewritten as (29).

3.3 The New Proposed Controller Design Steps

1) State-space related to the power system;
2) Determining the initial value (ϕ_1, ϕ_2, and ϕ_3);
3) Solving the linear matrix inequality (Eqs. (13) and (29)) and Γ_1, Γ_2, Γ_3, Γ_4, Γ_5, Γ_6, Γ_7, Γ_8, Γ_9, $\Gamma_{10}>0$ using YALMIP;
4) Are all linear matrix inequalities correct? (If they are correct go to step 5, if not go to step 2);

5) Obtaining $L_{n\times p}$, $K_{m\times n}$, $E_{n\times n}$, $S_{n\times n}$, $R_{n\times n}$ through Steps (2) and (3);
5) Determining N and M as $N = I$ and $M = I–RS$;
6) Obtaining the controller parameters via (23).
The proposed controller flowchart is shown in Fig. 5.

$$\begin{cases}\delta_2 < 0 & ,\varsigma^T \delta_2 \varsigma < 0\\ \varsigma > 0\end{cases} \tag{19}$$

$$\varsigma = \begin{bmatrix}\beta_1 & 0 & 0\\ 0 & I & 0\\ 0 & 0 & I\end{bmatrix}, \varsigma^T = \begin{bmatrix}\beta_1^T & 0 & 0\\ 0 & I & 0\\ 0 & 0 & I\end{bmatrix} \tag{20}$$

$$\delta_3 = \begin{bmatrix}\beta_1^T & 0 & 0\\ 0 & I & 0\\ 0 & 0 & I\end{bmatrix}\delta_2\begin{bmatrix}\beta_1 & 0 & 0\\ 0 & I & 0\\ 0 & 0 & I\end{bmatrix}$$

$$= \begin{bmatrix} \beta_1^T \bar{A}^T \beta_2 + \beta_2^T \bar{A} \beta_1 & \beta_2^T \bar{D} & \beta_1^T \begin{bmatrix} C_1^T(t) \\ \hat{C}^T D_{12}^T(t) \end{bmatrix} \\ \bar{D}^T \beta_2 & \gamma^2 I & 0 \\ \begin{bmatrix} C_1(t) & D_{12}(t)\hat{C} \end{bmatrix} \beta_1 & 0 & -I \end{bmatrix} < 0 \tag{21}$$

$$\delta_3 = \begin{bmatrix} A(t)R + RA^T(t) + M\hat{C}(t)B^T(t) & A(t) + RA^T(t)S + M\hat{C}^T(t)B^T(t)S + RC_2^T(t)\hat{B}^T(t)N^T + M\hat{A}^T(t)N^T & D(t) & RC_1^T(t) + M\hat{C}^T(t)D_{12}^T(t) \\ A^T(t) + SA(t)R + SB(t)\hat{C}M^T + N\hat{B}(t)C_2(t) + N\hat{A}M^T & A^T(t)S + SA(t) + N\hat{B}C_2(t)\hat{B}^T N^T & SD(t) & C_1^T(t) \\ D^T(t) & D^T(t)S & -\gamma^2 I & 0 \\ C_1(t)R + D_{12}(t)\hat{C}M^T & C_1(t) & 0 & -I \end{bmatrix} < 0 \tag{22}$$

$$\begin{cases}\hat{A} = N^{-1}(E - LC_2R - SAR - SBK)M^{-T}, \hat{B} = N^{-1}L\\ \hat{C} = KM^{-T}\end{cases} \tag{23}$$

$$\delta_3 = \begin{bmatrix} AR + RA^T + BK + K^T B^T & A + E^T & D & RC_1^T + K^T D_{12}^T \\ A^T + E & A^T S + SA + LC_2 + C_2^T L^T & SD & C_1^T \\ D^T & D^T S & -\gamma^2 I & 0 \\ C_1 R + D_{12}K & C_1 & 0 & -I \end{bmatrix} + o_1 + o_2 + o_3 + o_4 + o_5$$
$$+ o_6 + o_7 + o_8 + o_9 + o_{10} + o_{11} + o_{12} + o_{13} < 0$$

$$o_1 = \begin{bmatrix}\Delta AR + R\Delta A^T & 0 & 0 & 0\\ 0 & 0 & 0 & 0\\ 0 & 0 & 0 & 0\\ 0 & 0 & 0 & 0\end{bmatrix}, o_2 = \begin{bmatrix}\Delta BK + K^T\Delta B^T & 0 & 0 & 0\\ 0 & 0 & 0 & 0\\ 0 & 0 & 0 & 0\\ 0 & 0 & 0 & 0\end{bmatrix}, o_3 = \begin{bmatrix}0 & \Delta A & 0 & 0\\ \Delta A^T & 0 & 0 & 0\\ 0 & 0 & 0 & 0\\ 0 & 0 & 0 & 0\end{bmatrix},$$

$$o_4 = \begin{bmatrix}0 & R\Delta A^T S & 0 & 0\\ S\Delta A^T R & 0 & 0 & 0\\ 0 & 0 & 0 & 0\\ 0 & 0 & 0 & 0\end{bmatrix}, o_5 = \begin{bmatrix}0 & K^T\Delta B^T S & 0 & 0\\ S\Delta BK & 0 & 0 & 0\\ 0 & 0 & 0 & 0\\ 0 & 0 & 0 & 0\end{bmatrix}, o_6 = \begin{bmatrix}0 & R\Delta C_2^T L^T & 0 & 0\\ L\Delta C_2 R & 0 & 0 & 0\\ 0 & 0 & 0 & 0\\ 0 & 0 & 0 & 0\end{bmatrix},$$

$$o_7 = \begin{bmatrix}0 & 0 & \Delta D & 0\\ 0 & 0 & 0 & 0\\ \Delta D^T & 0 & 0 & 0\\ 0 & 0 & 0 & 0\end{bmatrix}, o_8 = \begin{bmatrix}0 & 0 & 0 & R\Delta C_1^T\\ 0 & 0 & 0 & 0\\ 0 & 0 & 0 & 0\\ \Delta C_1 R & 0 & 0 & 0\end{bmatrix}, o_9 = \begin{bmatrix}0 & 0 & 0 & K^T\Delta D_{12}^T\\ 0 & 0 & 0 & 0\\ 0 & 0 & 0 & 0\\ \Delta D_{12}K & 0 & 0 & 0\end{bmatrix},$$

$$o_7=\begin{bmatrix}0&0&\Delta D&0\\0&0&0&0\\\Delta D^T&0&0&0\\0&0&0&0\end{bmatrix},o_8=\begin{bmatrix}0&0&0&R\Delta C_1^T\\0&0&0&0\\0&0&0&0\\\Delta C_1R&0&0&0\end{bmatrix},o_9=\begin{bmatrix}0&0&0&K^T\Delta D_{12}^T\\0&0&0&0\\0&0&0&0\\\Delta D_{12}K&0&0&0\end{bmatrix},$$

$$o_{10}=\begin{bmatrix}0&0&0&0\\0&\Delta A^TS+S\Delta A&0&0\\0&0&0&0\\0&0&0&0\end{bmatrix},o_{11}=\begin{bmatrix}0&0&0&0\\0&L\Delta C_2+\Delta C_2^TL^T&0&0\\0&0&0&0\\0&0&0&0\end{bmatrix},o_{12}=\begin{bmatrix}0&0&0&0\\0&0&S\Delta D&0\\0&\Delta D^TS&0&0\\0&0&0&0\end{bmatrix},$$

$$o_{13}=\begin{bmatrix}0&0&0&0\\0&0&0&\Delta C_1^T\\0&0&0&0\\0&0&\Delta C_1&0\end{bmatrix},o=\begin{bmatrix}AR+RA^T+BK+K^TB^T&A+E^T&D&RC_1^T+K^TD_{12}^T\\A^T+E&A^TS+SA+LC_2+C_2^TL^T&SD&C_1^T\\D^T&D^TS&-\gamma^2I&0\\C_1R+D_{12}K&C_1&0&-I\end{bmatrix} \tag{24}$$

$$\sigma F\upsilon+\upsilon^TF^T\sigma^T\le\Gamma\sigma\sigma^T+\Gamma^{-1}\upsilon^T\upsilon,F^TF\le I \tag{25}$$

$$o_1=\sigma_1F\upsilon_1+\upsilon_1^TF^T\sigma_1^T\le\Gamma_1\sigma_1\sigma_1^T+\Gamma_1^{-1}\upsilon_1^T\upsilon_1,\ o_2=\sigma_2F\upsilon_2+\upsilon_2^TF^T\sigma_2^T\le\Gamma_2\sigma_2\sigma_2^T+\Gamma_2^{-1}\upsilon_2^T\upsilon_3$$

$$o_3=\sigma_3F\upsilon_3+\upsilon_3^TF^T\sigma_3^T\le\Gamma_3\sigma_3\sigma_1^T+\Gamma_3^{-1}\upsilon_3^T\upsilon_3,\ o_4=\sigma_4F\upsilon_4+\upsilon_4^TF^T\sigma_4^T\le\Phi_1\sigma_4\sigma_4^T+\Phi_1^{-1}\upsilon_4^T\upsilon_4$$

$$o_5=\sigma_5F\upsilon_5+\upsilon_5^TF^T\sigma_5^T\le\Phi_2\sigma_5\sigma_5^T+\Phi_2^{-1}\upsilon_5^T\upsilon_5,\ o_6=\sigma_6F\upsilon_6+\upsilon_6^TF^T\sigma_6^T\le\Phi_3\sigma_6\sigma_6^T+\Phi_3^{-1}\upsilon_6^T\upsilon_6$$

$$o_7=\sigma_7F\upsilon_7+\upsilon_7^TF^T\sigma_7^T\le\Gamma_4\sigma_7\sigma_7^T+\Gamma_4^{-1}\upsilon_7^T\upsilon_7,\ o_8=\sigma_8F\upsilon_8+\upsilon_8^TF^T\sigma_8^T\le\Gamma_5\sigma_8\sigma_8^T+\Gamma_5^{-1}\upsilon_8^T\upsilon_8$$

$$o_9=\sigma_9F\upsilon_9+\upsilon_9^TF^T\sigma_9^T\le\Gamma_6\sigma_9\sigma_9^T+\Gamma_6^{-1}\upsilon_9^T\upsilon_9,\ o_{10}=\sigma_{10}F\upsilon_{10}+\upsilon_{10}^TF^T\sigma_{10}^T\le\Gamma_7\sigma_{10}\sigma_{10}^T+\Gamma_7^{-1}\upsilon_{10}^T\upsilon_{10}$$

$$o_{11}=\sigma_{11}F\upsilon_{11}+\upsilon_{11}^TF^T\sigma_{11}^T\le\Gamma_8\sigma_{11}\sigma_{11}^T+\Gamma_8^{-1}\upsilon_{11}^T\upsilon_{11},\ o_{12}=\sigma_{12}F\upsilon_{12}+\upsilon_{12}^TF^T\sigma_{12}^T\le\Gamma_9\sigma_{12}\sigma_{12}^T+\Gamma_9^{-1}\upsilon_{12}^T\upsilon_{12}$$

$$o_{13}=\sigma_{13}F\upsilon_{13}+\upsilon_{13}^TF^T\sigma_{13}^T\le\Gamma_{10}\sigma_{13}\sigma_{13}^T+\Gamma_{10}^{-1}\upsilon_{13}^T\upsilon_{13}$$

$$\sigma_1=\begin{bmatrix}M_A\\0\\0\\0\end{bmatrix},\ \upsilon_1=\begin{bmatrix}N_AR&0&0&0\end{bmatrix},\ \sigma_2=\begin{bmatrix}M_B\\0\\0\\0\end{bmatrix},\ \upsilon_2=\begin{bmatrix}0&N_A&0&0\end{bmatrix}$$

$$\sigma_3=\begin{bmatrix}M_A\\0\\0\\0\end{bmatrix},\ \upsilon_3=\begin{bmatrix}0&N_A&0&0\end{bmatrix},\ \sigma_4=\begin{bmatrix}0\\SM_A\\0\\0\end{bmatrix},\ \upsilon_4=\begin{bmatrix}N_AR&0&0&0\end{bmatrix}$$

$$\sigma_5=\begin{bmatrix}0\\SM_B\\0\\0\end{bmatrix},\ \upsilon_5=\begin{bmatrix}N_BK&0&0&0\end{bmatrix},\ \sigma_6=\begin{bmatrix}0\\LM_{C_2}\\0\\0\end{bmatrix},\ \upsilon_6=\begin{bmatrix}N_{C_2}R&0&0&0\end{bmatrix}$$

$$\sigma_7=\begin{bmatrix}M_D\\0\\0\\0\end{bmatrix},\ \upsilon_7=\begin{bmatrix}0&0&N_D&0\end{bmatrix},\ \sigma_8=\begin{bmatrix}0\\0\\0\\M_{C_1}\end{bmatrix},\ \upsilon_8=\begin{bmatrix}N_{C_1}R&0&0&0\end{bmatrix}$$

$$\sigma_9=\begin{bmatrix}0\\0\\0\\M_{D_{12}}\end{bmatrix},\ \upsilon_9=\begin{bmatrix}N_{D_{12}}K&0&0&0\end{bmatrix},\ \sigma_{10}=\begin{bmatrix}0\\SM_A\\0\\0\end{bmatrix},\ \upsilon_{10}=\begin{bmatrix}0&N_A&0&0\end{bmatrix}$$

$$\sigma_{11}=\begin{bmatrix}0\\ LM_{C_2}\\ 0\\ 0\end{bmatrix},\ \upsilon_{11}=\begin{bmatrix}0 & N_{C_2} & 0 & 0\end{bmatrix},\ \sigma_{12}=\begin{bmatrix}0\\ SM_D\\ 0\\ 0\end{bmatrix},\ \upsilon_{12}=\begin{bmatrix}0 & 0 & N_D & 0\end{bmatrix}$$

$$\sigma_{13}=\begin{bmatrix}0\\ 0\\ 0\\ M_{C_1}\end{bmatrix},\upsilon_{13}=\begin{bmatrix}0 & N_{C_1} & 0 & 0\end{bmatrix},\ \bar{o}_1=\Gamma_1\sigma_1\sigma_1^T+\Gamma_1^{-1}\upsilon_1^T\upsilon_1,\ \bar{o}_2=\Gamma_2\sigma_2\sigma_2^T+\Gamma_2^{-1}\upsilon_2^T\upsilon_2$$

$$\bar{o}_3=\Gamma_3\sigma_3\sigma_3^T+\Gamma_3^{-1}\upsilon_3^T\upsilon_3,\quad \bar{o}_4=\Phi_1\sigma_4\sigma_4^T+\Phi_1{}^{-1}\upsilon_4^T\upsilon_4,\ \bar{o}_5=\Phi_2\sigma_5\sigma_5^T+\Phi_2{}^{-1}\upsilon_5^T\upsilon_5,\ \bar{o}_6=\Phi_3\sigma_6\sigma_6^T+\Phi_3{}^{-1}\upsilon_6^T\upsilon_6,$$
$$\bar{o}_7=\Gamma_4\sigma_7\sigma_7^T+\Gamma_4^{-1}\upsilon_7^T\upsilon_7,\quad \bar{o}_8=\Gamma_5\sigma_8\sigma_8^T+\Gamma_5^{-1}\upsilon_8^T\upsilon_8,\quad \bar{o}_9=\Gamma_6\sigma_9\sigma_9^T+\Gamma_6^{-1}\upsilon_9^T\upsilon_9,\quad \bar{o}_{10}=\Gamma_7\sigma_{10}\sigma_{10}^T+\Gamma_7^{-1}\upsilon_{10}^T\upsilon_{10},$$
$$\bar{o}_{11}=\Gamma_8\sigma_{11}\sigma_{11}^T+\Gamma_8^{-1}\upsilon_{11}^T\upsilon_{11},\ \bar{o}_{12}=\Gamma_9\sigma_{12}\sigma_{12}^T+\Gamma_9^{-1}\upsilon_{12}^T\upsilon_{12},\ \bar{o}_{13}=\Gamma_{10}\sigma_{13}\sigma_{13}^T+\Gamma_{10}^{-1}\upsilon_{13}^T\upsilon_{13} \tag{26}$$

$$\delta_3\le o+\sum_{i=1}^{13}\bar{o}_i=\delta_4<0 \tag{27}$$

$$\delta_4=o+\sum_{i=2}^{13}\bar{o}_i+\begin{bmatrix}\Gamma_1M_AM_A^T & 0 & 0 & 0\\ 0 & 0 & 0 & 0\\ 0 & 0 & 0 & 0\\ 0 & 0 & 0 & 0\end{bmatrix}+\begin{bmatrix}RN_A^T\\ 0\\ 0\\ 0\end{bmatrix}\Gamma_1^{-1}\begin{bmatrix}N_AR & 0 & 0 & 0\end{bmatrix}<0$$

$$\delta_4=\begin{bmatrix}o+\sum_{i=2}^{13}\bar{o}_i & \begin{bmatrix}RN_A^T\\ 0\\ 0\\ 0\end{bmatrix}\\ \begin{bmatrix}N_AR & 0 & 0 & 0\end{bmatrix} & -\Gamma_1\end{bmatrix}<0 \tag{28}$$

$$\delta_4=\begin{bmatrix}
\delta_{11_{n\times n}} & A+E^T & D & RC_1^T+KD_{12}^T & RN_A^T & K^TN_B^T & 0_{n\times1} & 0_{n\times1} & RN_{C_1}^T & KN_{D_{12}}^T & 0_{n\times1} & 0_{n\times1} & 0_{n\times1} & 0_{n\times1} & RN_A^T & 0_{n\times1} & K^TN_B^T & 0_{n\times1} & RN_{C_2}^T\\
A^T+E & \delta_{22_{n\times n}} & SD & C_1^T & 0_{n\times1} & 0_{n\times1} & N_A^T & 0_{n\times1} & 0_{n\times1} & 0_{n\times1} & SM_A & LM_{C_2} & SN_D & N_{C_1}^T & SM_A & 0_{n\times1} & SM_B & 0_{n\times1} & LM_{C_2} & 0_{n\times1}\\
D & D^TS & \delta_{33_{d\times d}} & 0_{d\times q} & 0_{d\times1} & 0_{d\times1} & N_D^T & 0_{d\times1} & 0_{d\times1} & 0_{d\times1} & 0_{d\times1} & 0_{d\times1} & 0_{d\times1} & 0_{d\times1} & 0_{d\times1} & 0_{d\times1} & 0_{d\times1} & 0_{d\times1} & 0_{d\times1} & 0_{d\times1}\\
C_1R+D_{12}K & C_1 & 0_{q\times d} & \delta_{44_{q\times q}} & 0_{q\times1} & 0_{q\times1} & 0_{q\times1} & 0_{q\times1} & 0_{q\times1} & 0_{q\times1} & 0_{q\times1} & 0_{q\times1} & 0_{q\times1} & 0_{q\times1} & 0_{q\times1} & 0_{q\times1} & 0_{q\times1} & 0_{q\times1} & 0_{q\times1} & 0_{q\times1}\\
N_AR & 0_{1\times n} & 0_{1\times d} & 0_{1\times q} & -\Gamma_1 & 0 & 0 & 0 & 0 & 0 & 0 & 0 & 0 & 0 & 0 & 0 & 0 & 0 & 0 & \\
N_BK & 0_{1\times n} & 0_{1\times d} & 0_{1\times q} & 0 & -\Gamma_2 & 0 & 0 & 0 & 0 & 0 & 0 & 0 & 0 & 0 & 0 & 0 & 0 & 0 & \\
0_{1\times n} & N_A & 0_{1\times d} & 0_{1\times q} & 0 & 0 & -\Gamma_3 & 0 & 0 & 0 & 0 & 0 & 0 & 0 & 0 & 0 & 0 & 0 & 0 & \\
0_{1\times n} & 0_{1\times n} & N_D & 0_{1\times q} & 0 & 0 & 0 & -\Gamma_4 & 0 & 0 & 0 & 0 & 0 & 0 & 0 & 0 & 0 & 0 & 0 & \\
N_{C_1}R & 0_{1\times n} & 0_{1\times d} & 0_{1\times q} & 0 & 0 & 0 & 0 & -\Gamma_5 & 0 & 0 & 0 & 0 & 0 & 0 & 0 & 0 & 0 & 0 & \\
N_{D_{12}}K & 0_{1\times n} & 0_{1\times d} & 0_{1\times q} & 0 & 0 & 0 & 0 & 0 & -\Gamma_6 & 0 & 0 & 0 & 0 & 0 & 0 & 0 & 0 & 0 & \\
0_{1\times n} & M_A^TS & 0_{1\times d} & 0_{1\times q} & 0 & 0 & 0 & 0 & 0 & 0 & -\Gamma_7 & 0 & 0 & 0 & 0 & 0 & 0 & 0 & 0 & \\
0_{1\times n} & M_{C_2}^TL^T & 0_{1\times d} & 0_{1\times q} & 0 & 0 & 0 & 0 & 0 & 0 & 0 & -\Gamma_8 & 0 & 0 & 0 & 0 & 0 & 0 & 0 & \\
0_{1\times n} & M_D^TS & 0_{1\times d} & 0_{1\times q} & 0 & 0 & 0 & 0 & 0 & 0 & 0 & 0 & -\Gamma_9 & 0 & 0 & 0 & 0 & 0 & 0 & \\
0_{1\times n} & N_{C_1} & 0_{1\times d} & 0_{1\times q} & 0 & 0 & 0 & 0 & 0 & 0 & 0 & 0 & 0 & -\Gamma_{10} & 0 & 0 & 0 & 0 & 0 & \\
0_{1\times n} & M_A^TS & 0_{1\times d} & 0_{1\times q} & 0 & 0 & 0 & 0 & 0 & 0 & 0 & 0 & 0 & 0 & -\Phi_1^{-1} & 0 & 0 & 0 & 0 & \\
N_AR & 0_{1\times n} & 0_{1\times d} & 0_{1\times q} & 0 & 0 & 0 & 0 & 0 & 0 & 0 & 0 & 0 & 0 & 0 & -\Phi_1 & 0 & 0 & 0 & \\
0_{1\times n} & M_B^TS & 0_{1\times d} & 0_{1\times q} & 0 & 0 & 0 & 0 & 0 & 0 & 0 & 0 & 0 & 0 & 0 & 0 & -\Phi_2^{-1} & 0 & 0 & \\
N_BK & 0_{1\times n} & 0_{1\times d} & 0_{1\times q} & 0 & 0 & 0 & 0 & 0 & 0 & 0 & 0 & 0 & 0 & 0 & 0 & 0 & -\Phi_2 & 0 & \\
0_{1\times n} & M_{C_2}^TL^T & 0_{1\times d} & 0_{1\times q} & 0 & 0 & 0 & 0 & 0 & 0 & 0 & 0 & 0 & 0 & 0 & 0 & 0 & 0 & -\Phi_3^{-1} & \\
N_{C_2}R & 0_{1\times n} & 0_{1\times d} & 0_{1\times q} & 0 & 0 & 0 & 0 & 0 & 0 & 0 & 0 & 0 & 0 & 0 & 0 & 0 & 0 & 0 & -\Phi_3
\end{bmatrix}<0 \tag{29}$$

4 Simulation

The dynamic controller values for the coordinated control of the LFC and SMES systems in the power system are presented in Appendix 2. Simulations were conducted under five scenarios to compare the performances of the proposed controller in the coordinated control of the LFC and SMES systems. In scenarios (1) and (2), the load and distributed generation resource disturbances act on the power system. In

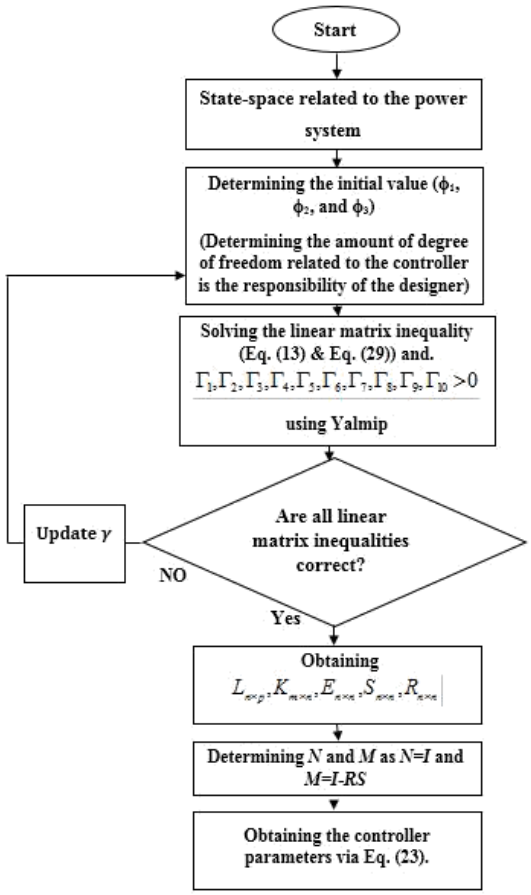

Fig. 5 The proposed controller flowchart.

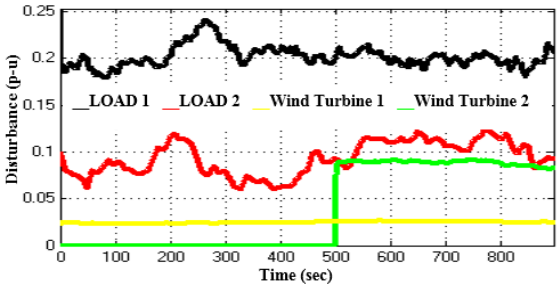

Fig. 6 The load and distributed generation resources (wind turbine) disturbances.

scenarios (3) and (4), the load and distributed generation resource disturbances are applied to the power system considering the uncertainty of various parameters. In scenario (5), stronger disturbances are applied to the power system.

Scenario (1): In this scenario, the load and distributed generation resources (wind turbine) disturbances are applied to the power system as depicted in Fig. 6. Fig. 7(a) shows the frequency response of the power system using the coordinated control method for LFC and SMES systems based on the new robust controller (Controller 1). The maximum frequency deviation resulting from the proposed method (Controller 1) is 0.0018Hz. Fig. 7(b) shows the frequency response of

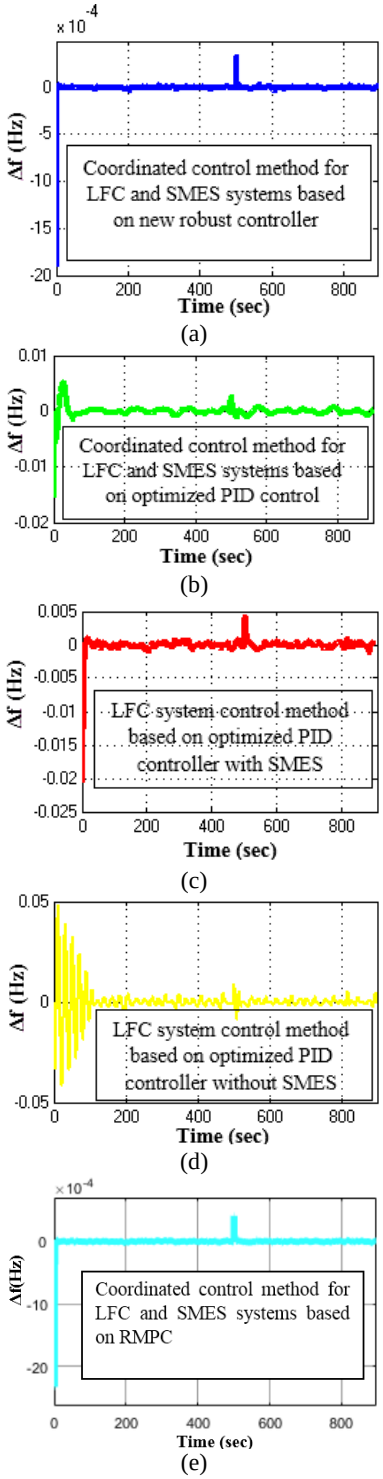

Fig. 6 a) The frequency response using the proposed controller for scenario (1), b) The frequency response using the coordinated control method for LFC and SMES systems based on the MSA-optimized PID controller for scenario (1), c) The frequency response using the LFC system control method based on MSA-optimized PID controller with SMES for scenario (1), d) The frequency response using the LFC system control method based on the optimized PID without SMES for scenario (1), and e) The frequency response using the coordinated control method for LFC and SMES systems based on RMPC controller for scenario (1).

the power system using the coordinated control method for LFC and SMES systems based on the MSA-optimized PID controller (Controller 2). The maximum frequency deviation in this method (Controller 2) is 0.0173Hz. Fig. 7(c) shows the frequency response of the power system using the LFC system control method based on MSA-optimized PID controller with SMES (Controller 3). The maximum frequency deviation in this method (Controller 3) is 0.021Hz. Fig. 7(d) shows the frequency response of the power system using the LFC system control method based on the optimized PID without SMES (Controller 4). The maximum frequency deviation using this method (Controller 4) is 0.0476Hz. Fig. 7(e) shows the frequency response of the power system using the coordinated control method for LFC and SMES systems based on the Robust Model Predictive control (RMPC) (Controller 5). The maximum frequency deviation in this method (Controller 5) is 0.0022Hz. According to the results of the first scenario, the proposed controller (Controller 1) has maximum frequency deviations less than other control methods (Controller 2, Controller 3, Controller 4, Controller 5). The settling time in the frequency response of the power system using controller 1 is 5 seconds. The settling time in the frequency response of the power system using controller 2 is 19 seconds. The settling time in the frequency response of the power system using controller 3 is 38 seconds. The settling time in the frequency response of the power system using controller 4 is 90 seconds. The settling time in the frequency response of the power system using controller 5 is 5.73 seconds. According to the results of scenario 1, controller 1 dampens the frequency deviations related to the power system in less time than other mentioned controllers (Controller 2, Controller 3, Controller 4, Controller 5).

Scenario (2): In this scenario, the load and distributed generation resources (wind turbine) disturbances are applied to the power system as depicted in Fig. 8. Fig. 9(a) shows the frequency response of the power system using the coordinated control method for LFC and SMES systems based on the new robust controller (Controller 1). The maximum frequency deviation resulting from the proposed method (Controller 1) is 0.0015 Hz. Fig. 9(b) shows the frequency response of the power system using the coordinated control method for LFC and SMES systems based on the MSA-optimized PID controller (Controller 2). The maximum

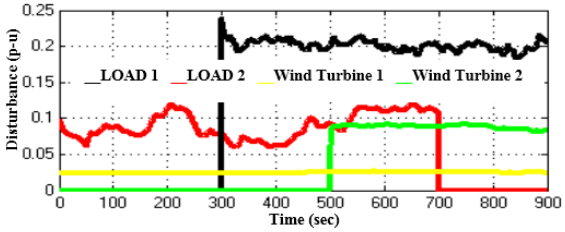

Fig. 8 The load and distributed generation resources (wind turbine) disturbances.

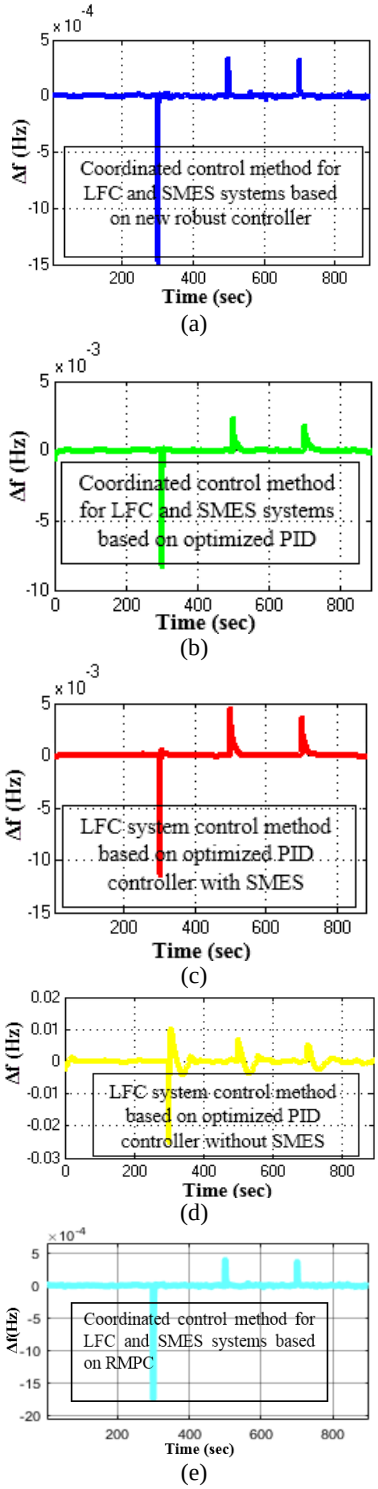

Fig. 9 a) The Frequency response using the proposed controller for scenario (2), b) The frequency response using the coordinated control method for LFC and SMES systems based on the MSA-optimized PID controller for scenario (2), c) The frequency response using the LFC system control method based on MSA-optimized PID controller with SMES for scenario (2), d) The frequency response using the LFC system control method based on the optimized PID without SMES for scenario (2), and e) The frequency response using the coordinated control method for LFC and SMES systems based on the RMPC controller for scenario (2).

frequency deviation in this method (Controller 2) is 0.0081 Hz. Fig. 9(c) shows the frequency response of the power system using the LFC system control method based on MSA-optimized PID controller with SMES (Controller 3). The maximum frequency deviation in this method (Controller 3) is 0.0129 Hz. Fig. 9(d) shows the frequency response of the power system using the LFC system control method based on the optimized PID without SMES (Controller 4). The maximum frequency deviation using this method (Controller 4) is 0.0256 Hz. Fig. 9(e) shows the frequency response of the power system using the coordinated control method for LFC and SMES systems based on the RMPC controller (Controller 5). The maximum frequency deviation in this method (Controller 5) is 0.0017 Hz. In this scenario, the settling time in the frequency response of the power system using controller 1 is 4.46 seconds. The settling time in the frequency response of the power system using controller 2 is 21 seconds. The settling time in the frequency response of the power system using controller 3 is 37 seconds. The settling time in the frequency response of the power system using controller 4 is 45 seconds. The settling time in the frequency response of the power system using controller 5 is 5.44 seconds. The simulation results in scenario (2) suggest that the proposed controller reduced the frequency deviations more than the other aforementioned control methods, and the frequency oscillations were dampened within a shorter period of time.

Scenario (3): In this scenario, the load and distributed generation resources (wind turbine) disturbances are applied to the power system as depicted in Fig. 8, and uncertainty is considered in system parameters (-25% inertia). Fig. 10(a) shows the frequency response of the power system using the coordinated control method for LFC and SMES systems based on the new robust controller (Controller 1). The maximum frequency deviation resulting from the proposed method (Controller 1) is 0.00163 Hz. Fig. 10(b) shows the frequency response of the power system using the coordinated control method for LFC and SMES systems based on the MSA-optimized PID controller (Controller 2). The maximum frequency deviation in this method (Controller 2) is 0.0106 Hz. Fig. 10(c) shows the frequency response of the power system using the LFC system control method based on MSA-optimized PID controller with SMES (Controller 3). The maximum frequency deviation in this method (Controller 3) is 0.0170 Hz. Fig. 10(d) shows the frequency response of the power system using the LFC system control method based on the optimized PID without SMES (Controller 4). The maximum frequency deviation using this method (Controller 4) is 0.0336 Hz. Fig. 10€ shows the frequency response of the power system using the coordinated control method for LFC and SMES systems based on the RMPC controller (Controller 5). The

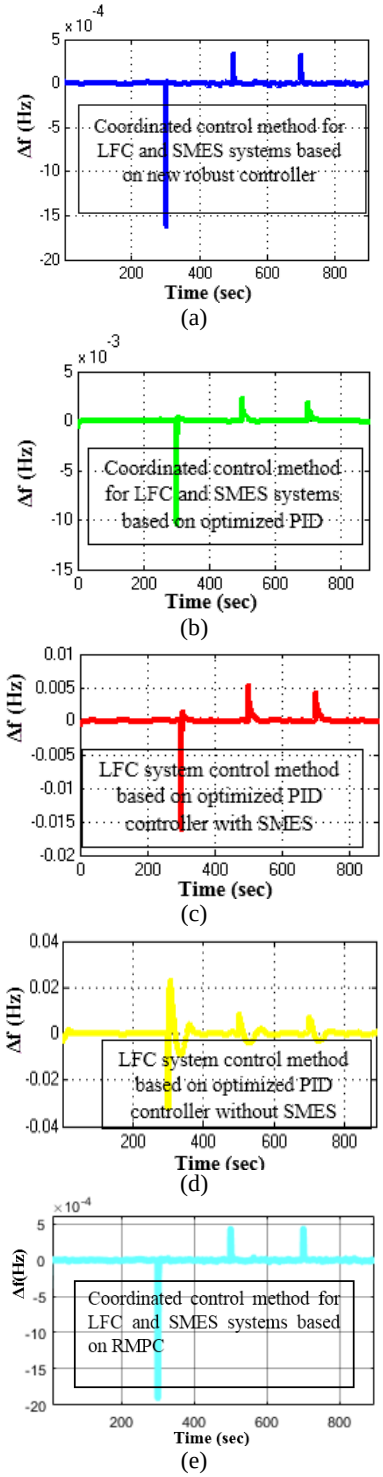

Fig. 10 a) The Frequency response using the proposed controller for scenario (3), b) The frequency response using the coordinated control method for LFC and SMES systems based on the MSA-optimized PID controller for scenario (3), c) The frequency response using the LFC system control method based on MSA-optimized PID controller with SMES for scenario (3), d) The frequency response using the LFC system control method based on the optimized PID without SMES for scenario (3), and e) The frequency response using the coordinated control method for LFC and SMES systems based on the RMPC controller for scenario (3).

maximum frequency deviation in this method (Controller 5) is 0.0019Hz. In this scenario, the settling time in the frequency response of the power system using controller 1 is 4.49 seconds. The settling time in the frequency response of the power system using controller 2 is 24 seconds. The settling time in the frequency response of the power system using controller 3 is 42 seconds. The settling time in the frequency response of the power system using controller 4 is 48 seconds. The settling time in the frequency response of the power system using controller 5 is 5.56 seconds. According to the simulation results in scenario (3), the proposed controller is very robust to disturbances and uncertainty parameters compared to the other control methods mentioned (LFC and SMES systems based on Moth Swarm Algorithm-optimized PID controller (Controller 2), the LFC system based on Moth Swarm Algorithm-optimized PID controller with SMES (Controller 3), LFC system based on optimized PID controller without SMES (Controller 4) and LFC and SMES systems based on the RMPC controller (Controller 5).

Scenario (4): In this scenario, the load and distributed generation resources (wind turbine) disturbances are applied to the power system as depicted in Fig. 8, and uncertainty is considered in system parameters (–50% inertia). Fig. 11(a) shows the frequency response of the power system using the coordinated control method for LFC and SMES systems based on the new robust controller (Controller 1). The maximum frequency deviation resulting from the proposed method (Controller 1) is 0.00172 Hz. Fig. 11(b) shows the frequency response of the power system using the coordinated control method for LFC and SMES systems based on the MSA-optimized PID controller (Controller 2). The maximum frequency deviation in this method (Controller 2) is 0.0157 Hz. Fig. 11(c) shows the frequency response of the power system using the LFC system control method based on MSA-optimized PID controller with SMES (Controller 3). The maximum frequency deviation in this method (Controller 3) is 0.0197 Hz. Fig. 11(d) shows the frequency response of the power system using the LFC system control method based on the optimized PID without SMES (Controller 4). The frequency changes have become unstable using this method (Controller 4). Fig. 11(e) shows the frequency response of the power system using the coordinated control method for LFC and SMES systems based on the RMPC controller (Controller 5). The maximum frequency deviation in this method (Controller 5) is 0.00205 Hz. In this scenario, the settling time in the frequency response of the power system using controller 1 is 4.49 seconds. The settling time in the frequency response of the power system using controller 2 is 25 seconds. The settling time in the frequency response of the power system using controller 3 is 46 seconds. The settling time in the frequency response of

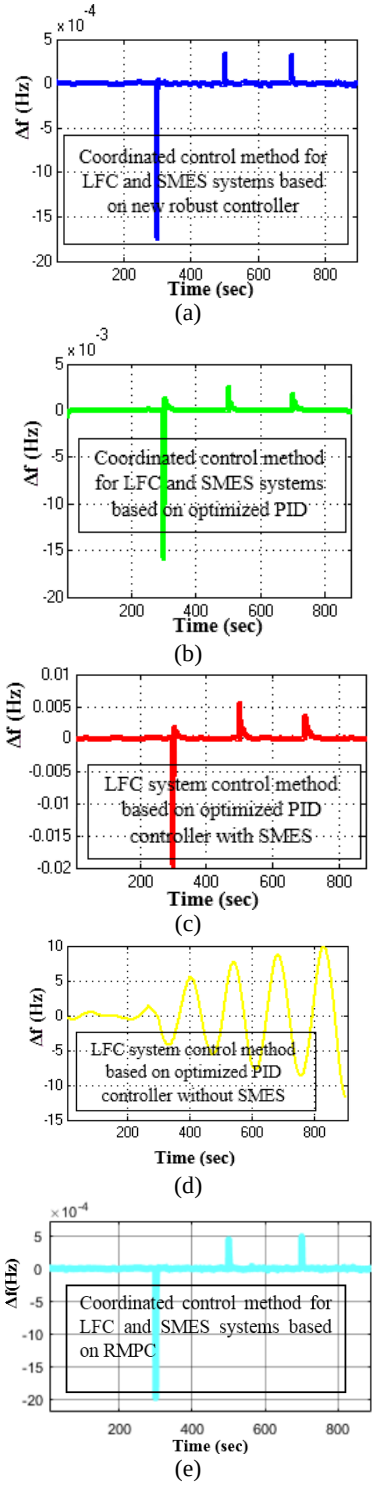

Fig. 11 a) The Frequency response using the proposed controller for scenario (4), b) The frequency response using the coordinated control method for LFC and SMES systems based on the MSA-optimized PID controller for scenario (4), c) The frequency response using the LFC system control method based on MSA-optimized PID controller with SMES for scenario (4), d) The frequency response using the LFC system control method based on the optimized PID without SMES for scenario (4), and e) The frequency response using the coordinated control method for LFC and SMES systems based on the RMPC controller for scenario (4).

the power system using controller 1 is not damped. The fourth control method is not robust to drastic changes in uncertainty related to the parameters of the power system. The settling time in the frequency response of the power system using controller 5 is 5.56 seconds. According to the simulation results in scenario (4), the proposed controller is very robust to disturbances and uncertainty parameters compared to the other control methods mentioned. Table 1 shows the results of different controllers in the power system.

Scenario 5: In this scenario, the load disturbances are pulsed into the power system as shown in Fig. 12. Fig. 13 shows the frequency response of the power system using different controllers. According to Fig. 13, using the proposed method, the frequency deviations related to the power system have been reduced and these fluctuations have accelerated over time. The proposed controller performs very well in reducing turbulence. The proposed controller performs well in weakening the disturbance.

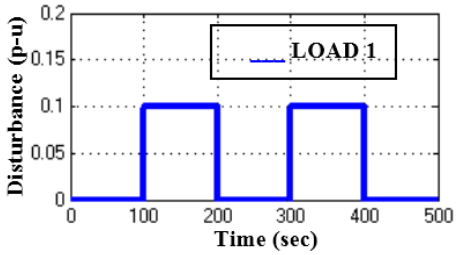

Fig. 12 The load disturbance.

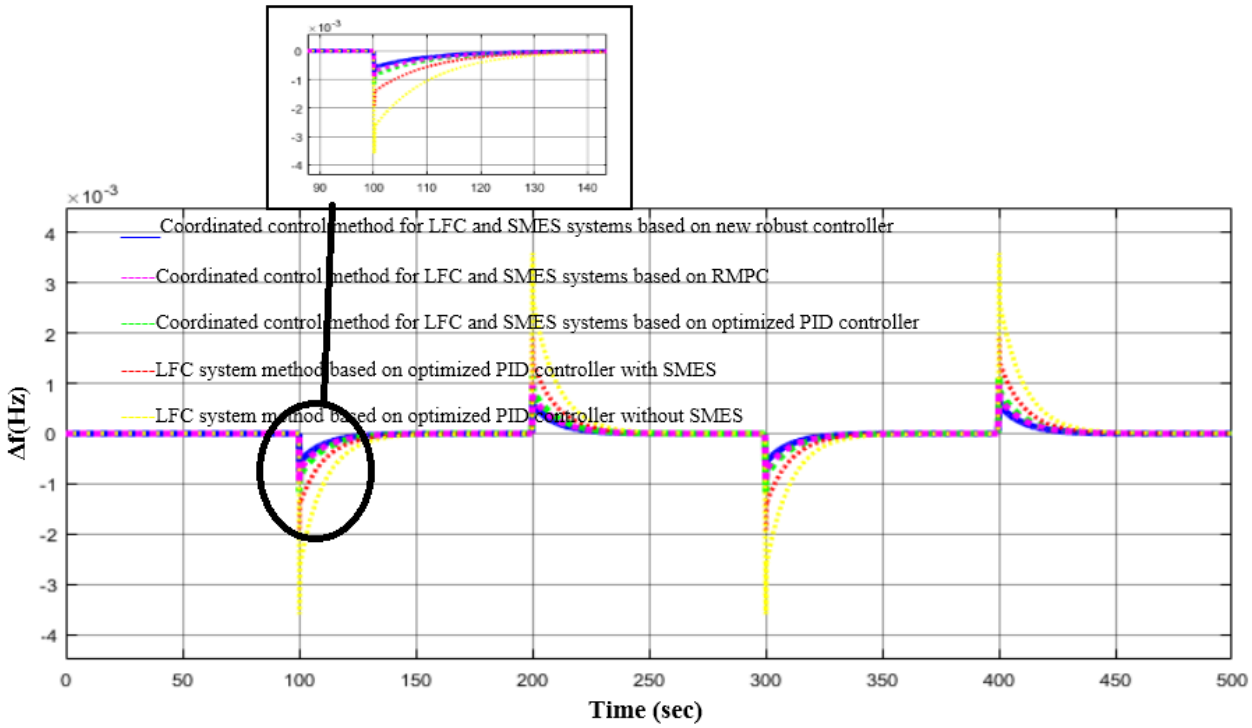

Fig. 13 The frequency response of the power system using different controllers.

Table 1 Results of different controllers in the power system.

Controller		Scenario 1	Scenario 2	Scenario 3	**Scenario 4**
Coordinated control method for LFC and SMES systems based on new robust controller	Maximum overshoot [pu]	0.0004	0.00037	0.00037	**0.00039**
	Maximum undershoot [pu]	0.0018	0.0015	0.00163	**0.00172**
	Settling time [sec]	5	4.46	4.49	**4.49**
Coordinated control method for LFC and SMES systems based on optimized PID controller [26]	Maximum overshoot [pu]	0.0042	0.002	0.0021	**0.0032**
	Maximum undershoot [pu]	0.0173	0.0081	0.0106	**0.0157**
	Settling time [sec]	19	21	24	**25**
LFC system control method based on optimized PID controller with SMES	Maximum overshoot [pu]	0.0044	0.005	0.0056	**0.0068**
	Maximum undershoot [pu]	0.021	0.0129	0.0170	**0.0197**
	Settling time [sec]	38	37	42	**46**
LFC system control method based on optimized PID controller without SMES	Maximum overshoot [pu]	0.0476	0.0100	0.0254	–
	Maximum undershoot [pu]	0.0466	0.0256	0.0336	–
	Settling time [sec]	90	45	48	–
Coordinated control method for LFC and SMES systems based on RMPC controller	Maximum overshoot [pu]	0.00046	0.00042	0.00047	**0.00052**
	Maximum undershoot [pu]	0.0022	0.0017	0.0019	**0.00205**
	Settling time [sec]	5.73	5.44	5.56	**5.56**

5 Conclusion

Today, the considerable penetration of the distributed generation resources in conventional power systems is undeniable. The presence of distributed generation resources has numerous advantages yet it increases the complexity of the control component of the power systems. Wind turbines are among the distributed generation resources that have penetrated power systems. The presence of wind turbines impairs the performance of the load-frequency system as these turbines rely on random wind speed. Hence, a robust control method is needed. In this paper, a coordinated control method for the LFC and SMES systems based on a new robust controller is designed. The new robust controller is based on the output feedback. The proposed method is converted into linear matrix inequalities using the Lyapunov criterion. A dynamic controller is designed for the power system by solving these inequalities in Yalmip. The results of the proposed controller are compared with the other controllers under different scenarios, revealing that this controller offers smaller maximum frequency overshoot and undershoot values and the frequency oscillations are dampened faster. Furthermore, the proposed controller shows a highly satisfactory performance in disturbance attenuation and it is robust under the uncertainty of the power system parameters.

Appendix 1

Table A1 Power system parameters [23-25].

Parameter	Value	Parameter	Value
R_1	2.5	m	0.5
R_2	2.5	T_d	5
R_3	1	T_1	0.4
β	1	T_2	0.4
T_w	1	T_3	90
T_h	6	H	5.7096
P_{n1}	0.2529	P_{n3}	0.1364
P_{n2}	0.6107	$P_{w,1}$	750 kW
$P_{w,2}$	3000 kW	D	0.028

Appendix 2

$$\hat{A}=\begin{bmatrix} -61.104 & 0.013333 & -0.00054096 & 0.001061 & -0.27094 & -0.1825 & -0.32574 & 0.09069 \\ -605.62 & -2.5882 & -0.084482 & -0.067504 & -7.096 & -5.7796 & -9.6682 & -0.65507 \\ -849.74 & -0.12281 & -0.6189 & -1.0204 & -9.9649 & -8.1163 & -13.574 & -0.92053 \\ -1259.1 & -0.18403 & -0.89815 & -2.306 & -14.774 & -12.037 & -20.115 & -1.3569 \\ -480.08 & -0.06948 & -0.066592 & -0.053456 & -7.2644 & -4.2273 & -7.6722 & -0.51673 \\ 473.16 & 0.068125 & 0.065512 & 0.052572 & 7.1546 & 4.1526 & 7.5633 & 0.50535 \\ -1.6731 & -0.00040 & -0.00023 & -0.000152 & -0.022112 & -0.018515 & -1.028 & -0.0055129 \\ -17122 & -2.4968 & -2.3828 & -1.9124 & -200.81 & -163.59 & -273.5 & -51.46 \end{bmatrix},$$

$$\hat{B}=\begin{bmatrix} -30638 \\ 40822 \\ 204356 \\ -73774 \\ 7653.5 \\ 5177 \\ 2938.9 \\ 273.44 \end{bmatrix},\quad \hat{C}^T=\begin{bmatrix} -0.059171 \\ -0.0086299 \\ -0.00835 \\ -0.00655 \\ -0.000694 \\ -0.00056536 \\ -0.00094523 \\ -0.00063797 \end{bmatrix}$$

References

[1] H. Shayeghi and A. Younesi, "An online Q-learning based multi-agent LFC for a multi-area multi-source power system including distributed energy resources," *Iranian Journal of Electrical and Electronic Engineering*, Vol. 13, No. 4, pp. 385–398, 2017.

[2] H. Abdi, M. P. Moghaddam, and M. H. Javidi, "A probabilistic approach to transmission expansion planning in deregulated power systems under uncertainties," *Iranian Journal of Electrical and Electronic Engineering*, Vol. 1, No. 3, pp. 43–52, 2005.

[3] M. Esmaili, H. A. Shayanfar, and N. Amjady, "Stochastic congestion management considering power system uncertainties," *Iranian Journal of Electrical and Electronic Engineering*, Vol. 6, No. 1, pp. 36–47, 2010.

[4] V. Rostampour, O. t. Haar, and T. Keviczky, "Distributed stochastic reserve scheduling in AC power systems with uncertain generation," *IEEE Transactions on Power Systems*, Vol. 34, No. 2, pp. 1005–1020, Mar. 2019.

[5] J. Johnson, J. Quiroz, R. Concepcion, F. Wilches-Bernal, and M. J. Reno, "Power system effects and mitigation recommendations for DER cyberattacks," *IET Cyber-Physical Systems: Theory & Applications*, Vol. 4, No. 3, pp. 240–249, 9 2019.

[6] F. Amiri and M. H. Moradi, "Designing a fractional order PID controller for a two-area micro-grid under uncertainty of parameters," *Iranian Journal of Energy*, Vol. 20, No. 4, pp. 49–78, 2018.

[7] F. Amiri and M. H. Moradi, "Designing a new robust control for virtual inertia control in the microgrid with regard to virtual damping," *Journal of Electrical and Computer Engineering Innovations*, Vol. 8, No. 1, pp. 53–70, 2020, 2020.

[8] G. Sharma, K. Narayanan, I. E., Davidson, and K. T. Akindeji, "Integration and enhancement of load frequency control design for diverse sources power system via DFIG based wind power generation and interconnected via parallel HVDC/EHVAC tie-lines," *International Journal of Engineering Research in Africa*, Vol. 46, pp. 106-124, 2020.

[9] N. Wang, J. Zhang, Y. He, M. Liu, Y. Zhang, C. Chen, and Y. Ren, "Load-frequency control of multi-area power system based on the improved weighted fruit fly optimization algorithm," *Energies*, Vol. 13, No. 2, p. 437, 2020.

[10] F. Amiri and A. Hatami, "Nonlinear Load frequency control of isolated microgrid using fractional order PID based on hybrid craziness-based particle swarm optimization and pattern search," *Journal of Iranian Association of Electrical and Electronics Engineers*, Vol. 17, No. 2, pp. 135–148, 2018.

[11] D. K. Lal and A. K. Barisal, "Combined load frequency and terminal voltage control of power systems using moth flame optimization algorithm," *Journal of Electrical Systems and Information Technology*, Vol. 6, No. 1, pp. 1–24, 2019.

[12] Y. Mi, X. Hao, Y. Liu, Y. Fu, C. Wang, P. Wang, and P. C. Loh, "Sliding mode load frequency control for multi-area time-delay power system with wind power integration," *IET Generation, Transmission & Distribution*, Vol. 11, No. 18, pp. 4644–4653, 2017.

[13] D. Qian, S. Tong, H. Liu, and X. Liu, "Load frequency control by neural-network-based integral sliding mode for nonlinear power systems with wind turbines," *Neurocomputing*, Vol. 173, pp. 875–885, 2016.

[14] X. Liu, Y. Zhang, and K. Y. Lee, "Coordinated distributed MPC for load frequency control of power system with wind farms," *IEEE Transactions on Industrial Electronics*, Vol. 64, No. 6, pp. 5140–5150, 2016.

[15] M. Ma, X. Liu, and C. Zhang, "LFC for multi-area interconnected power system concerning wind turbines based on DMPC," *IET Generation, Transmission & Distribution*, Vol. 11, No. 10, pp. 2689–2696, 2017.

[16] J. Yang, X. Sun, K. Liao, Z. He, and L. Cai, "Model predictive control-based load frequency control for power systems with wind-turbine generators," *IET Renewable Power Generation*, Vol. 13, No. 15, pp. 2871–2879, 2019.

[17] N. Nouri, A. A. Zamani, and S. M. Barakati, "Load frequency control with considering impact of wind turbine using a Fractional PID controller," in *Smart Grid Conference 2018 (SGC'18)*, Sanandaj, Iran, 2018.

[18] S. Berwal and B. Singh, "Load frequency control of a wind integrated power system using conventional PID & fuzzy PID controller," *International Research Journal of Engineering and Technology*, Vol. 6, No. 6, pp. 3702–3709, 2019.

[19] V. Gholamrezaie, M. G. Dozein, H. Monsef, and B. Wu, "An optimal frequency control method through a dynamic load frequency control (LFC) model incorporating wind farm," *IEEE Systems Journal*, Vol. 12, No. 1, pp. 392–401, Mar. 2018.

[20] A. Kumar and S. Suhag, "Effect of TCPS, SMES, and DFIG on load frequency control of a multi-area multi-source power system using multi-verse optimized fuzzy-PID controller with derivative filter," *Journal of Vibration and Control*, Vol. 24, No. 24, pp. 5922–5937, 2018.

[21] W. Guo, D. Li, F. Cai, C. Zhao, and L. Xiao, "Z-source-converter-based power conditioning system for superconducting magnetic energy storage system," *IEEE Transactions on Power Electronics*, Vol. 34, No. 8, pp. 7863–7877, Aug. 2019.

[22] Z. Zheng, X. Xiao, C. Huang, and C. Li, "Enhancing transient voltage quality in a distribution power system with SMES-based DVR and SFCL," *IEEE Transactions on Applied Superconductivity*, Vol. 29, No. 2, pp. 1–5, Mar. 2019.

[23] H. Alafnan, M. Zhang, W. Yuan, J. Zhu, J. Li, M. Elshiekh, and X. Li, "Stability improvement of DC power systems in an all-electric ship using hybrid SMES/battery," *IEEE Transactions on Applied Superconductivity*, Vol. 28, No. 3, pp. 1–6, Apr. 2018.

[24] M. Sharma, R. K. Bansal, and S. Prakash, "Robustness analysis of LFC for multi area power system integrated with SMES–TCPS by artificial intelligent technique," *Journal of Electrical Engineering & Technology*, Vol. 14, No. 1, pp. 97–110, 2019

[25] G. Magdy, G. Shabib, A. A. Elbaset, and Y. Mitani, "Optimized coordinated control of LFC and SMES to enhance frequency stability of a real multi-source power system considering high renewable energy penetration," *Protection and Control of Modern Power Systems*, Vol. 3, No. 1, pp. 1–15, 2018.

[26] G. Magdy, E. A. Mohamed, G. Shabib, A. A. Elbaset, and Y. Mitani, "SMES based a new PID controller for frequency stability of a real hybrid power system considering high wind power penetration," *IET Renewable Power Generation*, Vol. 12, No. 11, pp. 1304–1313, 2018.

[27] Y. Xie, L. Liu, Q. Wu, and Q. Zhou, "Robust model predictive control based voltage regulation method for a distribution system with renewable energy sources and energy storage systems," *International Journal of Electrical Power & Energy Systems*, Vol. 118, p. 105749, 2020

[28] M. H. Moradi and F. Amiri, "Virtual inertia control in islanded microgrid by using robust model predictive control (RMPC) with considering the time delay," *Soft Computing*, Vol. 25, pp. 6653–6663, 2021.

[29] M. Chilali, P. Gahinet, and C. Scherer, "Multiobjective output-feedback control via LMI optimization," *IEEE Transactions on Automatic Control*, Vol. 42, No. 7, pp. 896–911, Jul. 1997.

[30] F. Amiri and M. H. Moradi, "Angular speed control in a hybrid stepper motor using linear matrix inequality," *Computational Intelligence in Electrical Engineering*, In Press, 2021.

[31] H. Y. Li, X. J. Jing, and H. R. Karimi, "Output-feedback-based H∞ control for vehicle suspension systems with control delay," *IEEE Transactions on Industrial Electronics*, Vol. 61, No. 1, pp. 436–446, Jan. 2014.

[32] F. Amiri and M. H. Moradi, "Designing a new robust control method for AC servo motor," *Journal of Nonlinear Systems in Electrical Engineering*, Accepted, 2020.

F. Amiri was born in Ilam, Iran. He received the M.Sc. degree in Electrical Engineering from the University of Bu-Ali Sina in 2017. He is currently working toward the Ph.D. degree in Electrical Engineering at Bu-Ali Sina University. His research interests include dynamic and transient operation of power systems, control, microgrid, and renewable energy.

M. H. Moradi was born in Nowshahr, Mazandaran, Iran. He obtained his B.Sc., M.Sc., and Ph.D. from Sharif University of Technology, Tarbiat Modares University, and Strathclyde University in Glasgow, Scotland in 1991, 1993, and 2002, respectively. His research interests include new and green energy, microgrid modeling and control, DG location and sizing in power system, photovoltaic systems and power electronics, combined heat and power plant, power quality, supervisory control, fuzzy control